Studying the Dynamics of Coronavirus Replicative Structures

Marne C. Hagemeijer and Cornelis A.M. de Haan

Abstract

Coronaviruses (CoVs) generate specialized membrane compartments, which consist of double membrane vesicles connected to convoluted membranes, the so-called replicative structures, where viral RNA synthesis takes place. These sites harbor the CoV replication–transcription complexes (RTCs): multi-protein complexes consisting of 16 nonstructural proteins (nsps), the CoV nucleocapsid protein (N) and presumably host proteins. To successfully establish functional membrane-bound RTCs all of the viral and host constituents need to be correctly spatiotemporally organized during viral infection. Few studies, however, have investigated the dynamic processes involved in the formation and functioning of the (subunits of) CoV RTCs and the replicative structures in living cells. In this chapter we describe several protocols to perform time-lapse imaging of CoV-infected cells and to study the kinetics of (subunits of) the CoV replicative structures. The approaches described are not limited to CoV-infected cells; they can also be applied to other virus-infected or non-infected cells.

Key words Coronavirus, Nonstructural proteins, Live-cell imaging, Replication–transcription complex, Dynamics, Fluorescence recovery after photobleaching, Fluorescence loss in photobleaching

1   Introduction

Coronavirus (CoV) replicative structures are impressive multicomponent assemblies that consist of no less than 16 viral replicase proteins (the nonstructural proteins (nsps) [1–11]), the nucleocapsid (N) protein [10, 12–15], an as yet unknown number of host proteins, and an elaborate network of endoplasmic reticulum (ER)-derived double membrane vesicles and convoluted membranes [2, 4, 9, 16]. These "replication organelles" have been studied in lots of detail over the last few decades, generating a wealth of exciting information with respect to their composition, morphology, and functioning during the viral life cycle. Unfortunately one of the most, and perhaps unintentionally, overlooked areas is the real-time spatiotemporal dynamic behavior of the formation and functioning of the replicative structures

themselves but also the individual (membranous) associated components in living cells.

To study the dynamic processes underlying the formation and functioning of the CoV replicative structures and/or replication-associated proteins, one needs noninvasive means to visualize them in living cells. Recombinant CoVs expressing replicase proteins fused to fluorescent proteins (FPs) serve as an excellent tool to perform such real-time imaging studies in their native environment. Alternatively, these fluorescent fusion proteins may be expressed upon transfection of expression plasmids prior to infection, if desirable in combination with plasmids expressing host proteins fused to FPs. Using confocal laser scanning microscopy (CLSM) several live-cell imaging techniques can be employed to investigate the real-time kinetics of the replicative structures and its associated components. Once cells are infected with the recombinant FP-expressing CoVs, one can simply follow the fate of the replicative structures or its components over time, either under native or perturbed conditions, resulting in valuable spatiotemporal information with respect to the formation and behavior of the replicative structures and its associated components (*see* Fig. 1 for an example of a time-lapse experiment of MHV-nsp2GFP-infected LR7 cells). Alternatively, a (part of the) pool of FPs may be selectively and irreversibly photobleached and the temporal fate of the remaining non-bleached proteins may be followed [reviewed in [17–19]]. From the latter measurements parameters can be extracted, which among others reflect (the lack of) mobility
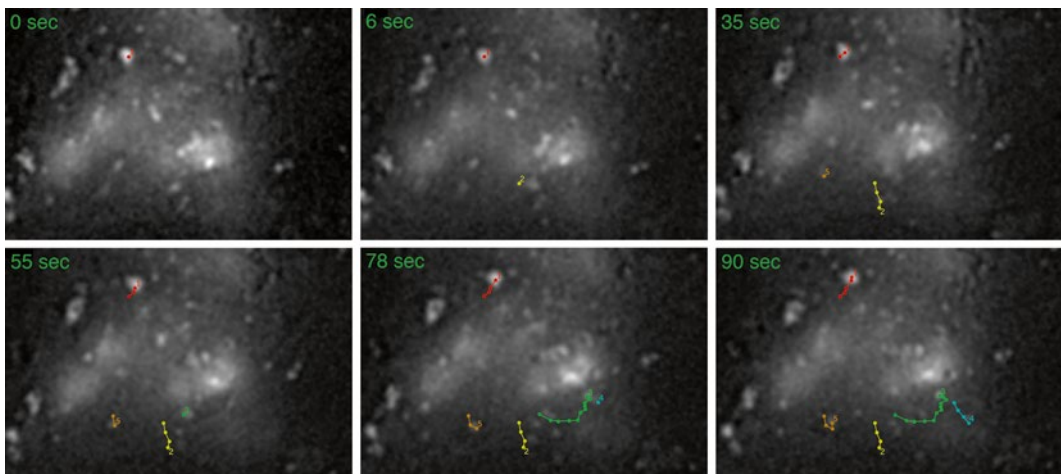

Fig. 1 Time-lapse imaging of MHV-nsp2GFP in LR7 cells. LR7 cells were infected with MHV-nsp2GFP [MHV expressing an nsp2-GFP fusion protein [21]] and at 6 h p.i. a time-lapse experiment was performed as described in Subheadings 3.1 and 3.2. Nsp2-GFP-positive foci were manually tracked over time using MtrackJ [22] and examples of the displacement of these structures have been indicated by the different *numbered* and *colored lines*
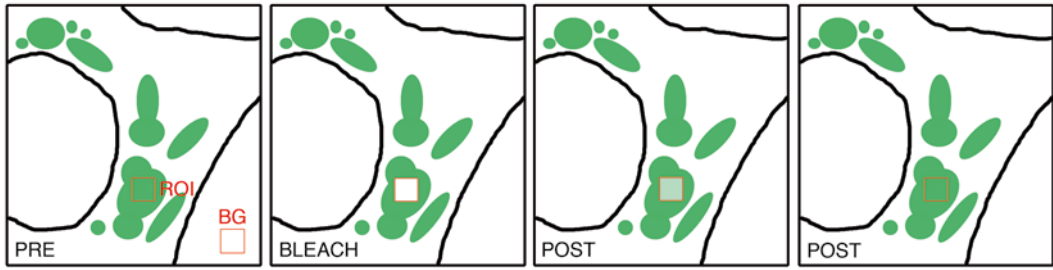
Fig. 2 Schematic overview of a FRAP experiment. A specific region of interest (ROI) targeting (part of) the FP-tagged replicative structure(s) is irreversibly photobleached and the recovery of fluorescence into the bleached area is monitored over time. In this example, the FP-tagged proteins are mobile as recovery of the fluorescence in the bleached area is observed [as has been previously observed for the MHV N protein [14]]. In the absence of recovery, the FP-tagged proteins are immobile [as has been observed for example for the MHV nsp2 protein [21]]. The *green structures* in the cell are a schematic representation of the replicative structures. *BG* background ROI for qualitative FRAP analysis
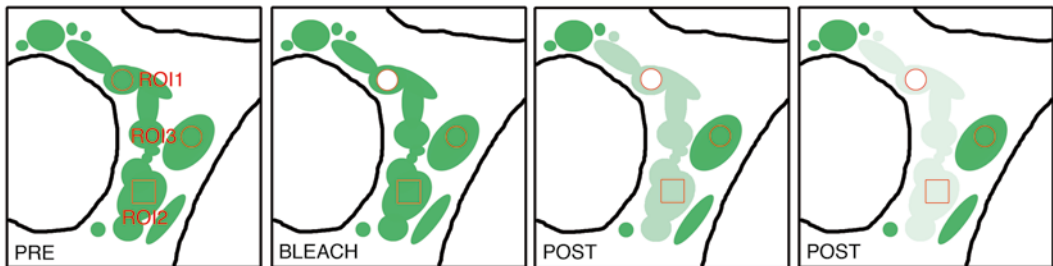

Fig. 3 Schematic overview of a FLIP experiment. The replicative structure(s) is repeatedly photobleached in ROI1 (*circle*) and the loss of fluorescence is monitored in ROI2 (*squared box*) or ROI3 (*circle*) over time. In this example the fluorescence of the FP-tagged structure is lost over time in ROI2, but not ROI3, indicating continuity between the membrane compartments of ROI1 and ROI2, but not between those of ROI1 and ROI3. Another cell in the field of view may be used to monitor/correct for photobleaching during the FLIP assay

[fluorescence recovery after photobleaching (FRAP)] or the (dis)continuity between different membrane compartments [fluorescence loss in photobleaching (FLIP)]. Figures 2 and 3 illustrate the principles of the FRAP and FLIP approaches, respectively, with typical fluorescence intensity graphs that can be obtained from these type of live-cell imaging experiments depicted in Fig. 4.

In this chapter we describe (1) a general protocol for setting up a time-lapse imaging experiment of CoV-infected cells to study the mobility of the replicative structures, followed by (2) two photobleaching approaches (FRAP and FLIP) to study the kinetics and continuity of the replicative structures and/or associated proteins, respectively and finally (3) how to analyze the quantitative kinetic data to obtain different parameters describing the dynamic behavior of the investigated structures/proteins in living cells.
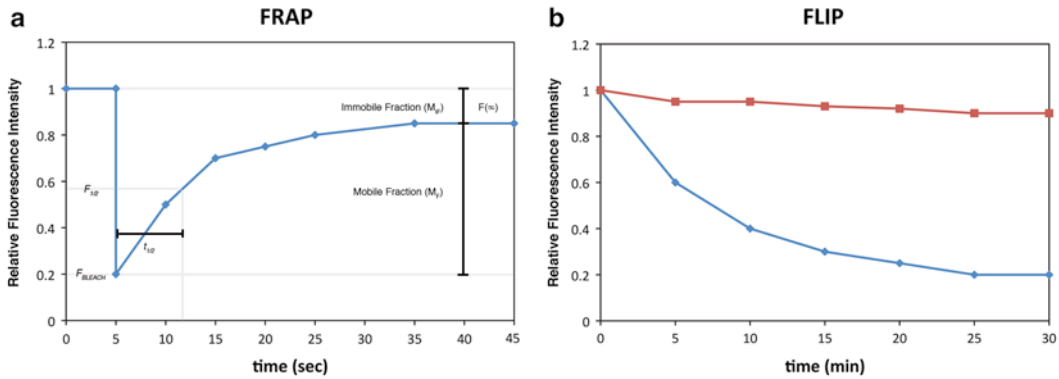
Fig. 4 Fluorescence graphs of typical FRAP and FLIP experiments. Two examples of typical fluorescence graphs when performing FRAP (*left graph*) or FLIP (*right graph*) experiments. (**a**) $F∞$: the plateau level reached at the end of the experiment, M_f: mobile fraction of the FP-tagged replicative structures, M_{IF}: the immobile fraction of the FP-tagged proteins present at the replicative structures, $t_{1/2}$: halftime of the recovery. (**b**) The decrease of fluorescence (*diamonds/blue line*) indicates that continuity between membrane compartments exists. If no or hardly any decrease is observed, the different membrane compartments are not continuous (for example ROI3 in Fig. 3). The *squares/red line* represents the loss of fluorescence of a control cell that is not photobleached and serves as a control that the observed loss of fluorescence is due to migration of FP-tagged proteins into the bleached area and not due to general photobleaching of the cell itself

Although, the live-cell imaging protocols described in this chapter uses CoV-infected cells, these approaches can easily be applied to other virus-infected or non-infected cells.

2   Materials

1. Mouse LR7 fibroblasts.

2. Cell culture medium: Dulbecco's Modified Eagle Medium (DMEM), 10 % fetal bovine serum (FBS), 100 IU/ml penicillin, 100 μg/ml streptomycin.

3. Imaging medium: DMEM without phenol-red, 10 % FBS and 25 mM HEPES pH 7.4.

4. Recombinant MHV(s) expressing viral FP-tagged proteins or wild-type MHV-A59.

5. Confocal Laser Scanning Microscope (CLSM) set up with a heated stage or environmental chamber.

6. Live-cell imaging clusters: 2- or 4-well Lab-Tek chamber slides or 35 mm MatTek #1.5 glass bottom dishes.

7. Plasmid DNA and transfection reagent (e.g., FuGENE 6 or Lipofectamine 2000) for (co)transfection of cells with a (viral or host) reporter plasmid prior to infection.

3   Methods

All procedures have to be performed at room temperature (RT) and under sterile conditions, unless otherwise stated in the text. We assume that the investigator has sufficient knowledge on how to operate a confocal microscope when following the live-cell imaging protocols described below.

3.1   Visualizing the CoV Replicative Structures and the Replicase Subunits

1. Plate mouse LR7 cells in culture medium on either Lab-Tek chamber slides or MatTek glass bottom dishes (#1.5 thickness) in such a density that 24–48 h after plating, the cells have reached 70–80 % confluency.

2. Prior to live-cell imaging infect the cells with recombinant FP-tagged MHV at a MOI of 10 for 1 h diluted in culture medium (infection medium) at 37 °C/5 % CO_2. Alternatively, transfect the cells with expression plasmids using standard protocols (e.g., by using FuGENE 6 or Lipofectamine 2000) 16–24 h prior to infection with recombinant FP-tagged or wild-type MHV.

3. After 1 h of infection, replace the infection medium with culture medium and allow incubation to continue at 37 °C/5 % CO_2.

4. At the preferred time point post infection (p.i.), replace the culture medium with pre-warmed (37 °C) imaging medium and transfer the Lab-Tek chamber slide or MatTek glass bottom dish to a [humidified (5 % CO_2)] heated incubation chamber (37 °C) on the microscope stage of the confocal microscope (*see* **Note 1**).

3.2   Real-Time Dynamics of the CoV Replicative Structures

1. After performing all the steps in Subheading 3.1 adjust the pinhole size of the CLSM to 1 airy unit (AU) and the scan area to 512 × 512 pixels with a bit depth of 12-bit. Do not apply any averaging during the acquisition process (*see* **Note 2**).

2. Turn on the required lasers to detect (and bleach, *see* Subheadings 3.3 and 3.4) the FP-tagged replicase protein(s) and adjust the laser power to a low percentage to prevent photobleaching of the FPs.

3. Start scanning the live cells using continuous acquisition and adjust the gain and offset for each laser channel (if applicable) to optimize the amount of fluorescent signal that the detectors will detect but without registering any oversaturated pixels in the field of view (*see* **Note 3**).

4. If the confocal microscope has the option to use an autofocus strategy to minimize (*x,y,z*) drift during the acquisition of the

time-lapse images, set up the autofocus strategy according to the manufacturer's instructions at this point.

5. Empirically determine the acquisition parameters, i.e., the number of time points to be imaged in a specific time interval that results in the acquisition of the maximum number of frames but the least amount of photobleaching of the cells.

6. Set up a time series using the parameters determined in **step 5** and start imaging the real-time dynamics of the CoV replicative structures.

7. Collect at least 5–10 individual time-lapse movies per experiment (Fig. 1).

3.3 FRAP of the CoV Replicative Structure (Subunits)

1. Perform **steps 1–5** as described in Subheading 3.2 but open the pinhole completely to acquire the maximum amount of fluorescent signal emitted from the whole cell (*see* **Note 4**).

2. Specify a region of interest (ROI) that targets (part of) the replicative structure that will be irreversibly photobleached (Fig. 2).

3. Set up a time-series that consists of (1) five pre-bleach images using the laser power established in **step 1**, (2) a photobleach event using 100 % laser power, and (3) an empirically determined number of post-bleach images (*see* **Note 5**).

4. Once the optimal bleaching and temporal parameters have been established perform approximately 5–10 FRAP experiments to acquire a sufficient number of data sets to extract qualitative FRAP parameters (*see* Subheading 3.5).

3.4 Continuity Between CoV Replicative Structures: FLIP

1. Perform **steps 1–5**, as described in Subheading 3.2, and open the pinhole completely.

2. Select a field of view, which contains at least two infected and/ or (co)transfected cells but preferably more (*see* **Note 6**).

3. Specify two ROIs in the targeted cell, one that will repeatedly be photobleached (Fig. 3, ROI1) and one where the loss of fluorescence intensity will be measured over time (Fig. 3, ROI2 and 3).

4. Set up an imaging protocol that includes (1) the acquisition of five pre-bleach images, (2) a 100 % laser power bleach event, and (3) the collection of ten post-bleach images. Steps (2) and (3) will have to be repeated for multiple cycles of which the number of cycles has to be determined empirically by the investigator. The cell(s) should be imaged during steps (1) and (3) using the acquisition settings as determined in **step 1**.

5. Perform approximately 5–10 FLIP experiments to acquire enough data sets to determine whether continuity between different membrane compartments exists.

3.5 Analysis of the Obtained Live-Cell Imaging Data

The majority of the commercial confocal microscope systems have excellent software packages installed on their workstations to perform (automated) analysis of the obtained data sets (e.g., softWoRx from Applied Precision or ZEN from Zeiss). If such software packages or automated approaches are not available, the open source program ImageJ [20] is a good alternative, from which qualitative parameters can be determined using the steps below as a general guideline.

1. After export from the quantitative (raw) data from the CLSM subtract the background fluorescence signal (F_{BG}) from the fluorescence signal from the bleached area (F_{ROI}) for each time point:

$$F_{ROI,BG}[t] = F_{ROI}[t] - F_{BG}[t] \tag{1}$$

2. Correct these measurements for any photobleaching that occurred over time during the image acquisition using the background-subtracted fluorescence intensity of the whole cell (F_{CELL}; *see* **Note 7**):

$$F_{ROI,CORR}[t] = F_{ROI,BG}[t] / (F_{CELL}[t] - F_{BG}[t]) \tag{2}$$

3. Normalize the obtained data to the fluorescent intensity of the first pre-bleach background-subtracted time point's fluorescent intensity (*see* **Note 7**):

$$F_{NORM}[t] = F_{ROI,CORR}[t] \times (F_{CELL}[0] - F_{BG}[0]) / F_{ROI,BG}[0] \tag{3}$$

4. Using the corrected and normalized fluorescence data, plot the fluorescence intensity in a particular region of interest (ROI) as shown in Fig. 4 (Fig. 4a, b are examples of a FRAP and FLIP graph, respectively).

5. The mobile fraction (M_f) can be determined using the generated fluorescence intensity plot(s) and the following formula:

$$M_f = (F[\infty] - F_{BLEACH}) / (1 - F_{BLEACH}) \tag{4}$$

6. The half-life of the bleached FPs ($t_{1/2}$) can be determined from the fluorescence intensity graph by determining $F_{1/2}$ (*see* **Note 8**):

$$F_{1/2} = (F[\infty] + F_{BLEACH}) / 2 \tag{5}$$

4 Notes

1. Whether or not CO_2 will be used during image acquisition depends on the microscope setup of the investigator, i.e., if an external CO_2 tank is connected to the incubation chamber. If not, HEPES-buffered culture medium can be used during

image acquisition. Both approaches have successfully been used in our laboratory.

2. Imaging at a high magnification of individual cells is preferable when performing time-lapse imaging of CoV replicative structures; the authors recommend using an oil immersion 40×/1.3NA or 63×/1.4NA objective.

3. Use the range indicator function of the confocal microscope to avoid imaging of oversaturated pixels, as data sets containing oversaturated pixels cannot be used for quantitative data analysis.

4. Opening the pinhole completely is important to ensure that the maximum amount of light emitted from the fluophores is collected and not only from a single focal plane.

5. When applying a single photobleach event of 100 % laser power, corresponding to the wavelength of the FP, does not result in a fluorescent intensity drop to background levels, the number of iterations should be increased. Once the recovery of the fluorescence in the bleached area reaches a plateau the acquisition of additional frames can be stopped.

6. During FLIP experiments the cell of interest is repeatedly photobleached at a high intensity laser power and therefore at least one control cell, i.e., a cell that is not photobleached, should be in the field of view to monitor whether loss of fluorescence is due to diffusion of the FPs and not due to photobleaching of the cell.

7. Correction for unwanted photobleaching is performed by using the fluorescent intensity (fluctuations) of the whole cell during the FRAP experiment. Such a control is not possible when performing FLIP as the loss of fluorescence is measured. Instead, the background-subtracted fluorescence of a whole non-bleached cell, which has been fitted to the equation $y(t) = \exp(-t/x)$, should be used for correction. For normalization of FLIP data use the following formula:
$F_{\mathrm{NORM}}[t] = F_{\mathrm{ROI,CORR}}[t] \times \left(1 / F_{\mathrm{ROI,BG}}[0]\right)$. We would like to recommend the investigator to consult reference [19] for more comprehensive in depth details on both FRAP and FLIP imaging approaches and data analysis.

8. Calculate the $F_{1/2}$ using formula (5) and determine the corresponding time point on the x-axis of the FR graph to determine $t_{1/2}$.

Acknowledgements

References

1. Deming DJ, Graham RL, Denison MR et al (2007) Processing of open reading frame 1a replicase proteins nsp7 to nsp10 in murine hepatitis virus strain A59 replication. J Virol 81:10280–10291

2. Goldsmith CS, Tatti KM, Ksiazek TG et al (2004) Ultrastructural characterization of SARS coronavirus. Emerg Infect Dis 10:320–326

3. Graham RL, Sims AC, Brockway SM et al (2005) The nsp2 replicase proteins of murine hepatitis virus and severe acute respiratory syndrome coronavirus are dispensable for viral replication. J Virol 79:13399–13411

4. Knoops K, Kikkert M, Worm SH et al (2008) SARS-coronavirus replication is supported by a reticulovesicular network of modified endoplasmic reticulum. PLoS Biol 6:e226

5. Oostra M, te Lintelo EG, Deijs M et al (2007) Localization and membrane topology of coronavirus nonstructural protein 4: involvement of the early secretory pathway in replication. J Virol 81:12323–12336

6. Prentice E, McAuliffe J, Lu X et al (2004) Identification and characterization of severe acute respiratory syndrome coronavirus replicase proteins. J Virol 78:9977–9986

7. Reggiori F, Monastyrska I, Verheije MH et al (2010) Coronaviruses Hijack the LC3-I-positive EDEMosomes, ER-derived vesicles exporting short-lived ERAD regulators, for replication. Cell Host Microbe 7:500–508

8. Shi ST, Schiller JJ, Kanjanahaluethai A et al (1999) Colocalization and membrane association of murine hepatitis virus gene 1 products and De novo-synthesized viral RNA in infected cells. J Virol 73:5957–5969

9. Snijder EJ, van der Meer Y, Zevenhoven-Dobbe J et al (2006) Ultrastructure and origin of membrane vesicles associated with the severe acute respiratory syndrome coronavirus replication complex. J Virol 80:5927–5940

10. Ulasli M, Verheije MH, de Haan CA et al (2010) Qualitative and quantitative ultrastructural analysis of the membrane rearrangements induced by coronavirus. Cell Microbiol 12:844–861

11. van der Meer Y, Snijder EJ, Dobbe JC et al (1999) Localization of mouse hepatitis virus nonstructural proteins and RNA synthesis indicates a role for late endosomes in viral replication. J Virol 73:7641–7657

12. Bost AG, Carnahan RH, Lu XT et al (2000) Four proteins processed from the replicase gene polyprotein of mouse hepatitis virus colocalize in the cell periphery and adjacent to sites of virion assembly. J Virol 74:3379–3387

13. Denison MR, Spaan WJ, van der Meer Y et al (1999) The putative helicase of the coronavirus mouse hepatitis virus is processed from the replicase gene polyprotein and localizes in complexes that are active in viral RNA synthesis. J Virol 73:6862–6871

14. Verheije MH, Hagemeijer MC, Ulasli M et al (2010) The coronavirus nucleocapsid protein is dynamically associated with the replication-transcription complexes. J Virol 84:11575–11579

15. Verheije MH, Raaben M, Mari M et al (2008) Mouse hepatitis coronavirus RNA replication depends on GBF1-mediated ARF1 activation. PLoS Pathog 4:e1000088

16. Gosert R, Kanjanahaluethai A, Egger D et al (2002) RNA replication of mouse hepatitis virus takes place at double-membrane vesicles. J Virol 76:3697–3708

17. Lippincott-Schwartz J, Snapp E, Kenworthy A (2001) Studying protein dynamics in living cells. Nat Rev Mol Cell Biol 2:444–456

18. Lippincott-Schwartz J, Altan-Bonnet N, Patterson GH (2003) Photobleaching and photoactivation: following protein dynamics in living cells. Nat Cell Biol S7–14

19. Bancaud A, Huet S, Rabut G et al (2010) Fluorescence perturbation techniques to study mobility and molecular dynamics of proteins in live cells: FRAP, photoactivation, photoconversion, and FLIP. Cold Spring Harb Protoc 2010, pdb top90

20. Rasband W (1997-2014) ImageJ. U.S. National Institutes of Health. Bethesda MD

21. Hagemeijer MC, Verheije MH, Ulasli M et al (2010) Dynamics of coronavirus replication-transcription complexes. J Virol 84:2134–2149

22. Meijering E, Dzyubachyk O, Smal I (2012) Methods for cell and particle tracking. Methods Enzymol 504:183–200